Inclusive production cross sections at 0° from reactions of ^{4}He + ^{12}C

A. Zarrella, J. Gauthier, K. Hagel, A. Jedele, A.B. McIntosh, A. Rodriguez Manso,
A. Wakhle, and S.J. Yennello

An experiment was conducted at the Cyclotron Institute which measured the cross section of the pionic fusion reaction $^{4}He + ^{12}C \rightarrow ^{16}N + \pi^{+}$ using a 55 MeV/nucleon ^{4}He beam. The Momentum Achromat Recoil Spectrometer (MARS) [1] was used to separate and collect the ^{16}N fusion residues at a silicon stack located at the spectrometer focal plane. While the search for pionic fusion events was the main goal of the experiment, various reaction products were also being collected. The range of measured magnetic rigidities spans from approximately 0.52 Tm to 0.69 Tm. This range was chosen as it is centered around the rigidity of $^{16}N^{7+}$ fragments traveling at the center of mass velocity of the colliding system. The cross sections reported in this document are for inclusive production and only consider fragments that are accepted into the spectrometer entrance which has a 9 msr solid angle centered at 0° with respect to the beam axis.

The cross sections have all been calculated using the thin target approximation given in Equation 1 where N is the yield of the detected species, Φ is the total integrated beam flux, ρ_{areal} is the areal density of the carbon target, and σ is the cross section.

$$N = \Phi \rho_{areal} \sigma \quad (1)$$

The beam current was constantly monitored using the event rate on the silicon stack at the MARS focal plane. This event rate was then calibrated using periodic Faraday cup measurements at the target position. The areal density of the target was determined using the energy lost in the foil by a ^{16}O beam. The particle identification (PID) process for the silicon stack is shown in Fig. 1. Panel (a) shows the first step of the PID where spots are identified in the E_{tot} vs. Y-position PID space. The Y-position is correlated with the mass-to-charge ratio of the species such that each of the clearly separated spots corresponds to particles with a particular mass and charge state. The rectangular PID gates are shown overlaid on this figure with the spot identifications noted. After this stage of identification, however, isobars with the same charge state ($^{12}B^{5+}$ and $^{12}C^{5+}$, for instance) are not separated. Panel (b) shows the second stage of PID for events inside the A = 12, Q = 5+ E_{tot} vs Y-position gate. This step uses the energy deposited in the dE component of the silicon stack versus the thickness of the dE silicon at the point where the particle was incident on the detector. This process was necessary because the thickness of the dE silicon was extremely non-uniform. As Fig. 1 (b) shows, this process produces good elemental PID separation between ^{12}B and ^{12}C. The PID gates are also overlaid and labeled.

Once the PID process was established, it is possible to begin considering particle yields. These yields, however, must be modified by various experimental efficiencies. Before the pionic fusion experiment, a beam of $^{16}O^{7+}$ was used to determine the transport efficiency of MARS for our residues of interest when their rigidity exactly matches the central rigidity of the MARS setting and was found to be 26%. Of course, not all transported particles are exactly at the central rigidity of the spectrometer. This

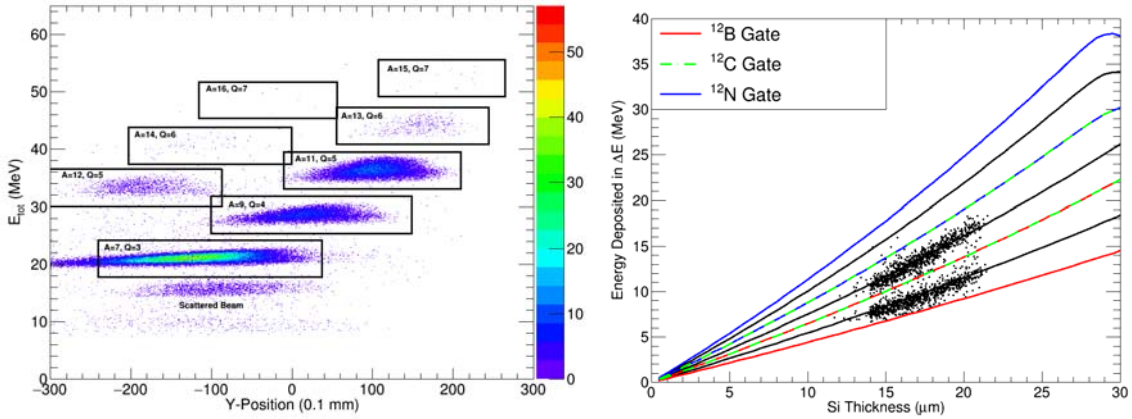

FIG. 1. (a) The Etot vs. Y-position PID plot collected while MARS was tuned for 0.5829 Tm. The vertical axis is the total measured kinetic energy in MeV and the horizontal axis is the Y-position in units of 0.1 mm. Each of the spots corresponds to species with the same mass and charge state and the rectangular PID gates are overlaid with the spot identifications noted. (b) The dE Energy vs. Si Thickness PID figure for the data inside the A = 12, Q = 5 gates from panel (a). The vertical axis is the energy deposited in the dE silicon in MeV and the horizontal axis is the thickness of the dE silicon in microns at the point where the particle hits the silicon stack. The black lines are SRIM predictions for (bottom to top) ^{12}B, ^{12}C and ^{12}N and the colored curves represent the PID gates in this space.

results in a reduction in the transmission efficiency as the particle's rigidity moves away from the central value. This effect, which will be called the Bρ window efficiency was determined using the measured shapes of the energy distributions of the various species. It was determined that this Bρ efficiency is 51%, meaning that around half of the particles with a rigidity inside the tuned MARS window are not transported to the focal plane. The live time of the data acquisition was being measured throughout the experiment and was always above 90%. There is also a detection efficiency associated with the charge state distribution of the residues of interest. Due to the limited width of the MARS Bρ measurement region, the experiment was only sensitive to a single charge state for each residue species. A semi-empirical formula [2] was used to calculate the expected charge state distribution for the residues leaving the ^{12}C target. The yields were then integrated over the charge distributions to produce a charge state integrated cross section.

As a comparison to the measured data, 64 million Gemini deexcitations of ^{16}O compound nuclei were simulated with a flat distribution of spins from 0ħ to 7ħ, the critical angular momentum for complete fusion in the reacting system [3]. The cooled fragments were then boosted into the lab frame and passed through a MARS filter which simulates the angular acceptance of the spectrometer and the rigidity selection. In order to translate the simulated particle yields so that they can be compared to the measured data, the number of ^{11}B fragments from the simulation was scaled to the measured cross section of ^{11}B and all of the simulated species were scaled by the same factor. Viewed in this way, the species-to-species trends can be compared to the measured results.

Fig. 2 shows the measured cross sections for all of the identified species in the experiment shown in closed circles and the scaled Gemini results in open circles. Species with the same number of protons, Z, are connected by solid lines in the cases of the data and dashed lines in the cases of the simulation.

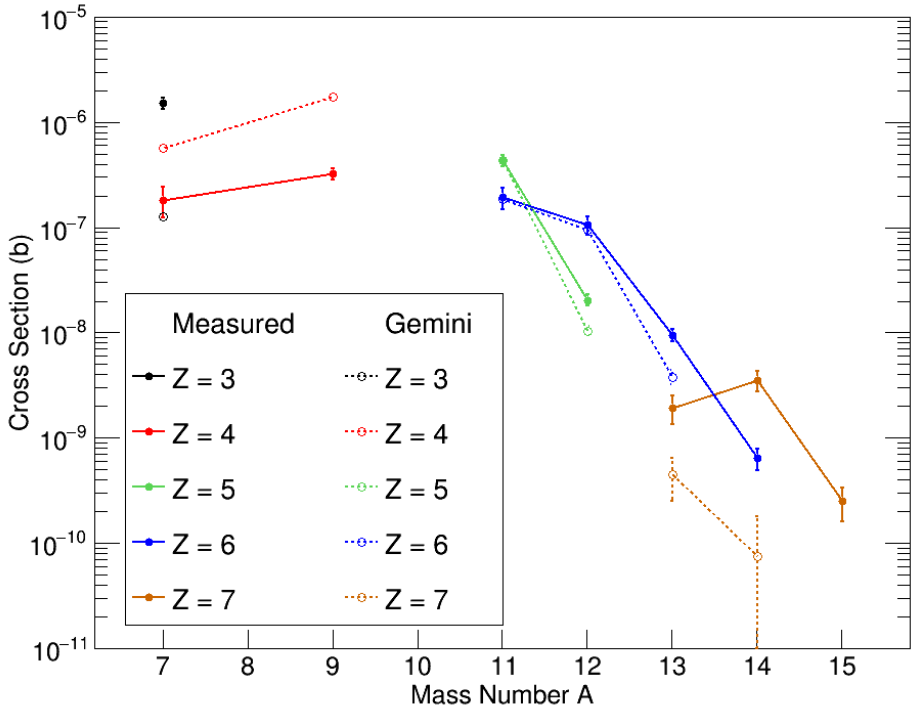

FIG. 2. The Bρ-integrated production cross sections for all species identified at the MARS focal plane during the pionic fusion experiment. The vertical axis is the cross section in barns and the horizontal axis is the particle mass number. The full circles are the measured cross sections and the open circles are the predictions from Gemini deexcitations of the compound nucleus. All species sharing the same proton number are connected with lines, solid for the measured data and dashed for the Gemini results.

The vertical axis is the cross section in barns and the horizontal axis is the species' mass number. The error bars on the measured data are produced by a detailed accounting of the uncertainties associated with the various efficiency corrections, the statistical uncertainties, and the PID uncertainties. The error bars on the Gemini results are produced by the addition in quadrature of the statistical uncertainties and the difference between the species yield at 0ħ spin and at 7ħ spin. This provides a conservative accounting for the non-triangular distribution of spins that were run. However, as is clear from the relative size of the error bars on the Gemini results, the statistical uncertainties dominate in the cases where the error bars are larger than the points. Note that the experimental and simulated values for ^{11}B are identical by definition since it was chosen for the scaling.

The experimental cross sections shown have been integrated over the range of investigated Bρs, 0.52 Tm to 0.69 Tm. The Gemini simulation fairly successfully reproduces the production trends in the mass range from A = 11 to A = 14 to within an order of magnitude in nearly every case. It is not as successful, though, in the A = 7 to A = 9 range. This is likely because the fragments larger than A = 11 are being produced through a similar set of mechanisms with a significant contribution from fusion-evaporation reactions. The lighter species may be resulting from different mechanisms such as pick-up

reactions or incomplete fusion. If this is the case, it is not surprising that the lighter species' productions do not track with the heavier products.

[1] R.E. Tribble *et al*., Nucl. Instrum. Methods Phys. Res. **A285**, 441 (1989).
[2] G. Schiwietz and P.L. Grande, Nucl. Instrum. Methods Phys. Res. **B175-177**, 125 (2001).
[3] W.W. Wilcke, *et al*., Data and Nuclear Data Tables **25**, 389 (1980).